Joint Pathology Center
Veterinary Pathology Services

WEDNESDAY SLIDE CONFERENCE 2021-2022

C o n f e r e n c e 4

15 September 2021

CASE I: 16855 (JPC 4157763)

Signalment: 2-year-old, female, Montana Tropical, (*Bos taurus*), bovine

History:
Two of 341 animals presented with swelling of the nose and lips (hippo face) and chest edema. These animals were being fed in a native field.

Gross Pathology: Inspection of the carcass revealed that no other organs except the head were involved.

Grossly, on the dorsal surface of tongue there are raised firm nodules and plaques, between 0.5 and 2 cm in diameter. Soft tissues of mandible especially pharyngo-laryngeal lymph nodes, salivary glands, lips, nostrils and tonsils were swelled and contained whitish nodules when incised.

Laboratory results:
Actinobacillus lignieresii were cultured.

Microscopic Description:
Histopathological examination of the skin and nasal soft tissues showed a thickened epidermis with scarring of the dermis and multiple pyogranulomas in the deep dermis.

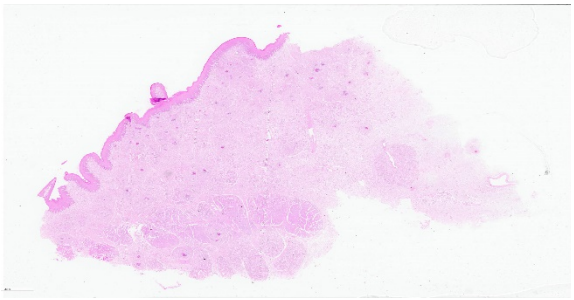

Figure 1-1: Nasal mucosa, ox. A section of nasal mucosa is submitted for examination (mucosa at left). Within the submucosa, numerous inflammatory nodules with a brightly eosinophilic center are present. (HE, 5X)

Within the lesions there were macrophages, epithelioid and multi-nucleated inflammatory giant cell and distinct rosettes of slender clubs with gram-negative coccobacilli at their center.

Contributor's Morphologic Diagnoses:
Rhinitis pyogranulomatous, bovine

Contributor's Comment:
Actinobacillosis is a sporadic infectious animal disease caused by the gram-negative bacilli *Actinobacillus lignieresii*. It is a common commensal inhabitant of the ruminant oral cavity. The bacteria can cause infection by invading adjacent soft tissues after the development of a penetrating wound.[4]
The genus *Actinobacillus* has remained relatively obscure until recently. In part, this

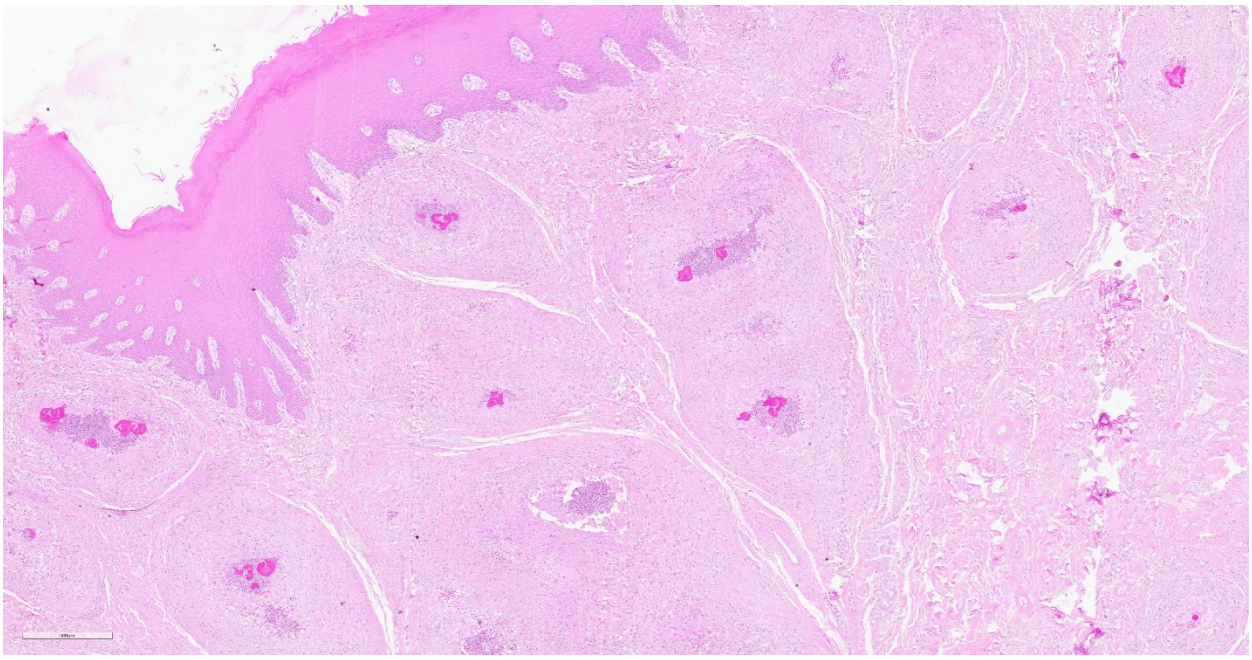

Figure 1-2: Nasal mucosa, ox. Higher magnification of the submucosa, which contains numerous often coalescing pyogranulomas centered on brightly eosinophilic Splendore-Hoeppli material. The overlying mucosa is normal. (HE, 75X)

must be due to their having been no recognized medical pathogen in the group to provoke research interest. The type species, *A. lignieresii*, has been recognized for many years as the cause of actinobacillosis in cattle and sheep. Latterly, the group has been growing with the recognition of *A. actinomycetemcomitans* as a significant cause of periodontal disease and the transfer from *Haemophilus* of *A. pleuropneumoniae*, an economically significant cause of respiratory disease in the pig. Through intense research interest focused on these two species, a much improved understanding of the bacteria has been acquired.[7]

The infection is characterized as a pyogranulomatous inflammation of the tongue, but also soft tissues as lymph nodes, other digestive tract localization and skin.[5] In our case, the inflammation spreads to the lips, palate, nostrils and nasal cavity. Because of that, the animal face assumed the aspect called "hippopotamus face".

Contributing Institution:
Regional Diagnostic Laboratory, Veterinary Faculty; Federal University of Pelotas.
96010-900 Pelotas, RS, Brazil.
https://wp.ufpel.edu.br/lrd/

JPC Diagnosis:
Nasal mucosa: Rhinitis, pyogranulomatous, chronic, multifocal to coalescing, moderate, with Splendore-Hoeppli material

JPC Comment:
Actinobacillus lignieresii was first identified as a pathogen by Lignierès and Spitz in South America during the early 20th century. A member of the family Pasteurellaceae, *A. lignieressii* is a commensal inhabitant of the upper digestive tract of ruminants and sporadically causes disease in cattle, sheep, goats, and rarely in other species. The condition is commonly associated with coarse poor-quality feed which is thought to cause traumatic inoculation; however other

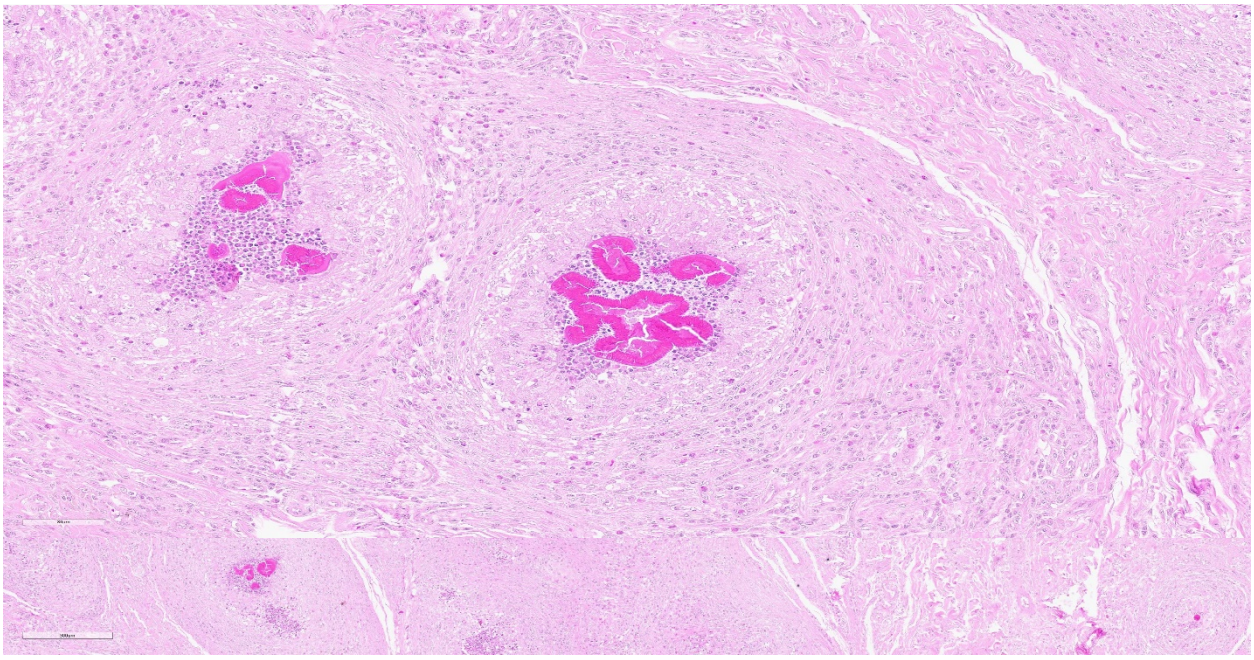

Figure 1-3: Nasal mucosa, ox. High magnification of pyogranulomas surrounding Splendore Hoeppli material. The thick layer of epithelioid macrophages surrounds the necrotic neutrophils and aggregated antigen-antibody complexes. (HE, 180X)

potential predisposing factors may include oral lesions secondary to viral infection, stress, and immunosuppression.[1]

In cattle, sheep, and goats, pyogranulomas caused by *A. lignieresii* most commonly occur in the soft tissues of the head and oral cavity and less often in other locations such as the forestomaches, lungs, and skin. Tongue lesions occur most often in cattle, commonly at the lingual groove, whereas sheep tend to develop lesions in the cutaneous and soft tissues of the lips and cheeks.[3] This is likely due to differences in food prehension between species, with cattle primarily using the tongue whereas small ruminants predominantly utilize the lips. Regardless of species, the lesion is characterized by chronic pyogranulomatous inflammation with marked fibrosis resulting in progressive interference of prehension and mastication of feed, eventually resulting in loss of condition and may ultimately result in starvation.[3] When the tongue is involved, it often becomes enlarged, firm, immobile, and may protrude from the mouth, resulting in the term "wooden tongue". Involvement of other organs, generally the skin or lymph nodes has been regarded as "atypical" or cutaneous actinobacillosis.[3] Draining lymph nodes, including the parotid, submandibular, and reropharyngeal lymph nodes may be involved, resulting in regional lymphadenitis. Severe cases may result in esophageal and airway compression, potentially resulting in dyspnea and/or ruminal tympany.[3]

On cut surface, pyogranulomas are grossly visible as small, soft yellow or orange masses that often contain "sulfur" granules.[1] Histologically, these granules correspond "club

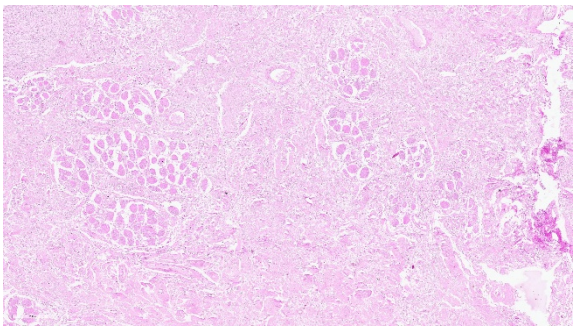

Figure 1-4: Nasal mucosa, ox. There is diffuse fibrosis of the nasal mucosa which has infiltrated the underlying atrophic skeletal muscle. (HE, 100X)

colonies" composed of gram negative coccobacilli surrounded by dense radiating eosinophilic club shaped Splendore-Hoeppli material. Club colonies are then surrounded by neutrophils, macrophages, and multi-nucleated giant cells. The surrounding reactive fibrous stroma and/or granulation tissue is further expanded by lymphocytes and plasma cells.[8]

Upon examination of previously described gross lesions, *Actinomyces bovis* should be considered as a leading differential diagnosis, although *Nocardia sp.,* and tuberculosis should also be considered. *A. bovis* is a gram positive, non-acid fast filamentous bacterium that frequently forms sulfur granules. Although this pathogen is typically associated with chronic osteomyelitis ("lumpy jaw" or actinomycosis), it may involve soft tissues.[1] *Nocardia sp.* is also a gram positive filamentous bacteria, but in contrast to *A. bovis*, *Nocardia sp.* are variably acid-fast and not typically associated with formation of sulfur granules. In Argentina, 14% of the lesions diagnosed macroscopically as tuberculosis by meat inspectors at slaughterhouses were actually actinobacillosis or actinomycosis. Therefore, actinobacillosis should be considered as differential in the diagnosis of tuberculosis and the importance of pursuing histologic and microbiologic examinations of compatible gross lesions for pathologic and etiologic confirmation.[1]

The moderator discussed use of the mnemonic "YAACSS-NT" (or "SSTAACY-N") as a memory aid when developing a differential diagnosis for genera commonly associated with the formation of large colonies. These genera include *Yersinia, Actinomyces, Actinobacillus, Corynebacterium, Streptococcus, Staphylococcus, Trueperella,* and occasionally *Nocardia.* It is important to state this list is not all-inclusive and other genera may also form colonies.

Many participants were unaware of the term "hippo face", a term which has been used in a scientific paper to describe the clinical manifestation of diffuse lesions affecting on the lips, palate, pharynx, nasal pits and face, which result in a unique "hippopotamus-like" appearance, much in the same manner as "wooden tongue".[10] A similar lesion caused by *Mannheimia granulomatis* has been described affecting the muzzles of white-tailed deer and mule deer.[5]

References:

1. Caffarena RD, Rabaza A, Casaux L, et al. Natural lymphatic ("atypical") actinobacillosis in cattle caused by Actinobacillus lignieresii. *J Vet Diagn Invest*. 2018;40(2):218-225.
2. Fenwick BW, Woolums AR. Pasteurellaceae: Actinobacillus. In: McVey DS, Kennedy M, Chenappa MM, eds. *Veterinary Microbiology*, 3rd Ed. Ames, IA: John Wiley and Sons. 2013:108-114.
3. Henton MM, Van Der Lugt JJ. Acintobacillus ignieresii infections. In: Coetzer JAW, Tustin RC, eds. *Infectious Diseases of Livestock*, 2nd Ed. Cape Town, South Africa: Oxford University Press Southern Africa. 2004:1648-1650.
4. Kasuya K, Manchanayake T, Uenoyama K, et al. Multifocal suppurative granuloma caused by Actinobacillus lignieresii in the peritoneum of a beef steer. *J Vet Med Sci*. 2017;79(1):65-67.
5. Keel MK, Keeler S, Brown J, et al. Granulomatous Inflammation of the Muzzle in White-Tailed Deer (*Odocoileus virginianus*) and Mule Deer (*Odocoileus hemionus*) Associated With *Mannheimia granulomatis*. *Vet Pathol*. 2020;57(6):838-844.
6. Margineda CA, Odriozola E, Moreira AR et al. Atypical actinobacillosis in

bulls in Argentina: granulomatous dermatitis and lymphadenitis. *Pesq Vet Bras*. 2014;44(1):1-5.
7. Relun A, Cesbron N, Bourdeau P, et al. Atypical actinobacillosis affecting hind limbs and lungs in a single beef cattle herd. *J Vet Intern Med*. 2019;44(1):297-401.
8. Rycroft AN, Garside LH. Actinobacillus species and their role in animal disease. *Vet J*. 2000;159(1):18-46.
9. Scheid HV, Estima-Silva P, Monteiro FL, et al. Actinobacillosis outbreak in cattle with clinical manifestation of hippopotamus-like face. *Pesq Vet Bras*. 2020;40(5):355-359.
10. Uzal F, Plattner BL, Hostetter JM. Alimentary system. In: Maxie MG, ed. *Jubb, Kennedy, and Palmer's Pathology of Domestic Animals*, 6th ed. St' Louis, Missouri: Elsevier; 2016: Vol 2: 18-19.

CASE II: 401-20 (JPC 4154112)

Signalment:
A 4-month old, neutered male, British Shorthair cat (*Felis catus)*

History:
The cat was adopted two weeks prior to presentation and kept mostly indoors. The owner reported a sudden onset of intermittent unsteady gait, polydipsia and polyuria.

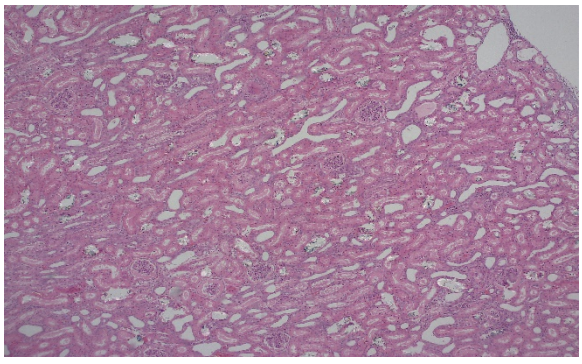

Figure 2-1: Kidney and brain, cat: A section of kidney and cerebrum are submitted for examination. There are several small subcapsular renal cysts, but no other discernable lesion at subgross magnification. (HE, 5X)

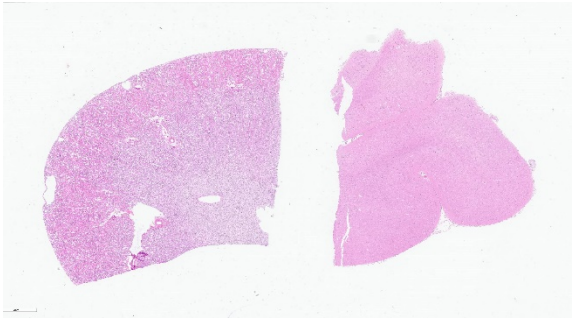

Figure 2-2: Kidney, cat: Diffusely, numerous tubules contain prismatic crystals within their lumina. (HE, 100X) (Photo courtesy of: Faculty of Veterinary and Agricultural Sciences, The University of Melbourne, 250 Princes Highway, Werribee Vic 3030, https://www.u-vet.com.au/)

Subsequently the cat had seizures. The animal was euthanized given a poor response to treatment.

Gross Pathology:
Both kidneys were slightly enlarged with cut surface bulging out.

Laboratory results:
Serum biochemistry revealed;

- Moderate azotaemia: creatinine: 330 µmol/L (ref 53-141 µmol/L), urea: 21mmol/L (ref 5.7-11.8 mmol)
- Increased liver enzymes: ALT: 469 U/L (ref 12-115 U/L), AST 161 U/L (ref: 0-32 U/L)
- Inadequate USG: 1.015 (ref 1.035-1.060)
- Severe metabolic acidosis: low blood HCO3 9.2 mmol/L (ref 22.0-24.0 mmol/L)

Microscopic Description:
Brain: Multifocally throughout the brain but most pronounced in the rostral cerebral cortex and the cerebellum, the walls of small-caliber blood vessels contain deposits of birefringent, transparent to slightly baso-phillic crystals at times arranged in sheaves, prisms and rosettes when illuminated with linearly polarized light (consistent with

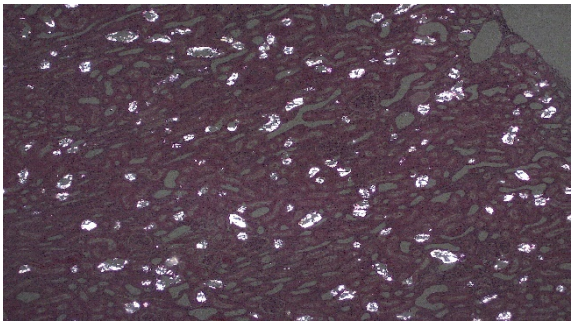

Figure 2-3: Kidney, cat: Polarized light demonstrate the extent of crystals within tubules. (HE, 100X) (Photo courtesy of: Faculty of Veterinary and Agricultural Sciences, The University of Melbourne, 250 Princes Highway, Werribee Vic 3030, https://www.u-vet.com.au/)

calcium oxalate crystals). Multifocally perivascular spaces (Virchow-Robin space) are mildly expanded and sometimes the affected vessels are lined by a swollen endothelium. Within the cerebellum there are also perivascular accumulations of small numbers of lymphocytes.

Kidney: Multifocally, proximal tubules are ectatic and often lined by degenerate and/or necrotic epithelium characterized by loss of cellular details with hypereosinophilia and pyknosis. The lumen of tubules often bears eosinophilic flocculent to hyalinzied (casts). Frequently within proximal tubular lumina and randomly in medullary tubules are deposits of birefringent, transparent to slightly basophilic crystals arranged in sheaves, prisms and rosettes when illuminated with linearly polarized light. Within the inters-titium there are also multifocal aggregates of neutrophils and lymphocytes.

Contributor's Morphologic Diagnoses:
Brain: Mild to moderate, multifocal, acute, crystal-induced vasculopathy

Kidney: Severe, multifocal, acute, tubular degeneration and necrosis with abundant intratubular calcium oxalate crystals and mild, multifocal, subacute interstitial nephritis.

Contributor's Comment:
Ethylene glycol (EG) is a colorless, odorless, slightly viscous dihydride alcohol with a sweet taste. It is an active constituent in automotive antifreeze solutions.[5] EG is highly toxic to human and animals and incidents of EG toxicity have been reported mainly via ingestion. [1,5,7] Once ingested EG is rapidly absorbed by the gastrointestinal system and hematogenously distributed to different tissues.[5] EG metabolism begins with gastric mucosal alcohol dehydrogenase and occurs primarily in the liver through serial oxidation by alcohol dehydrogenase and aldehyde dehydrogenase. [5] EG is considered to be two to five times more acutely toxic to humans and cats than to other animal species on a body weight basis. [1,5]

Ethylene glycol and its toxic metabolites including glycolic acid and oxalic acid play a deleterious role at the cellular level and predominantly involves the central nervous, cardiopulmonary and renal systems. During first 12 hours after acute oral exposure EG is progressively and rapidly metabolized resulting in accumulation of glycolic acids in blood manifesting severe anion gap metabolic acidosis.[1,5,7] Within 24 to 72 hours there may be evidence of precipitation of calcium oxalate crystals in target tissues

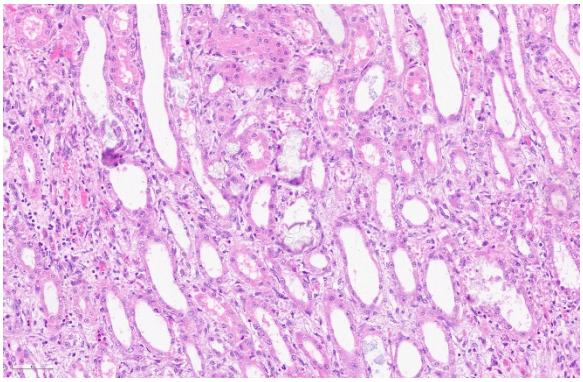

Figure 2-4: Kidney, cat: Calcium oxalate crystals often result in tubulorrhexis, resulting in incipient interstitial fibrosis and inflammation. (HE, 400X)

including kidneys, brain, heart and lungs. [3,5] Deposition of oxalic acids as calcium oxalate may also predispose to hypocalcemia. Thus, multisystemic toxicity is considered to be mostly due to metabolites which are highly toxic compared to their parent compound.

The mechanism of acute EG toxicity on the central nervous system is not well described. The direct effect of EG on acute exposure is high glycolate concentration along with crystalline deposits of calcium oxalate in blood vessels in the brain. These have been correlated with depressed activity of central nervous system. [1,2,3,5] Human studies have demonstrated that the deep grey matter nuclei of the basal ganglia, being metabolically more active than the remaining brain parenchyma are affected first by these metabolites, as well as by the associated hypoxia and acidosis.[5,6] The deposition of calcium oxalate crystals within the vasculature is likely to produce further edema and damage to the deep grey matter nuclei and adjacent white matter.[3,6] To this end, in the present case deposits of oxalate crystals are more pronounced in rostral cerebral cortex and cerebellum and basal ganglia and adjacent white matter appear to be unaffected.

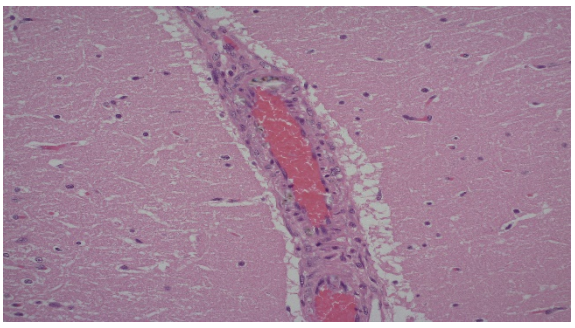

Figure 2-5: Cerebrum, cat: Calcium oxalate crystals are present within the walls of cerebral veins. (HE, 400X) (Photo courtesy of: Faculty of Veterinary and Agricultural Sciences, The University of Melbourne, 250 Princes Highway, Werribee Vic 3030, https://www.u-vet.com.au/)

Renal damage due to EG toxicity is correlated with acid metabolites of ethylene glycol, which can cause acute tubular necrosis, primarily of the proximal tubules. Deposition of calcium oxalate crystals, also primarily in proximal tubule epithelium, contributes to the renal parenchymal toxicity.[5] During acute EG toxicity kidneys may be enlarged with sharper cortico-medullary demarcations with histologically pathognomonic calcium oxalate crystals predominantly in proximal tubules.[1,7] Rarely deposition of calcium oxalate in the kidneys secondary to hyperoxaluria can be due to a mutation in the alanine: glyoxylate aminotransferase (AGT) gene or in the glyoxylate reductase (GRHPR) gene. The latter is described as an inherited disease in cats but polymerase chain reaction (PCR) failed to detect such a mutation in this case.[4] Ethylene glycol toxicity is suspected here with a suspicion that a disgruntled ex-partner of the owner may have been the source, but this is entirely speculative.

Contributing Institution:
Faculty of Veterinary and Agricultural Sciences
The University of Melbourne
250 Princes Highway
Werribee Vic 3030
https://www.u-vet.com.au/

JPC Diagnosis:
1. Kidney, tubules: Degeneration and necrosis, with numerous intratubular oxalate crystals and tubulorrhexis.

2. Cerebrum, vessels: Rare intramural oxalate crystals.

JPC Comment:
The contributor provides an excellent review of the pathogenesis, clinical progression, gross and histologic features associated with ethylene glycol toxicity.

In addition to ethylene glycol, conference participants discussed additional causes of oxalate nephrosis in various species, which include both primary and secondary (acquired) causes. Primary oxalate nephrosis is rare, and occurs as the result of catabolism of certain amino acids and vitamin C, resulting in the formation of endogenous oxalate crystals. Secondary oxalate nephrosis is more common and may occur due to pyridoxine (vitamin B6) deficiency, methoxyflurane anesthesia, ingestion of oxalate containing plants such as *Halogeton glomeratus, Sarcobatus vermiculatus* (greasewood), *Rheum rhaponticum* (rhubarb leaves), *Oxalis cernua* (soursob) and *Rumex (*sorrel and dock), or as the result of severe liver disease resulting in impaired oxalate metabolism.[2]

The moderator also discussed nephrotoxicity due to ingestion of food contaminated with melamine and cyanuric acid, which also results in the formation of crystals within renal tissue. Nephrotoxicity due to melamine -cyanuric acid results in the formation of gold-to-brown circular crystals with radiating spokes in the distal nephron that stain with oil red O. In contrast, oxalate crystals are concentrated in the proximal tubules and will stain with von Kossa. In addition, oxalate nephrosis is often associated with prominent hypocalcemia whereas serum calcium is usually normal in cases of melamine-cyanuric acid toxicity.[2]

In addition to having an interesting pathogenesis, this entity is also connected to a remarkable historical event arising from a medication known as "Elixir Sulfanilamide" in 1948.

Initially synthesized in 1908, sulfanilamide is an antibiotic that was commonly prescribed either in tablet or powder form. In 1948, a salesman for the S. E. Massengill Co., in Bristol, TN, reported a demand for the

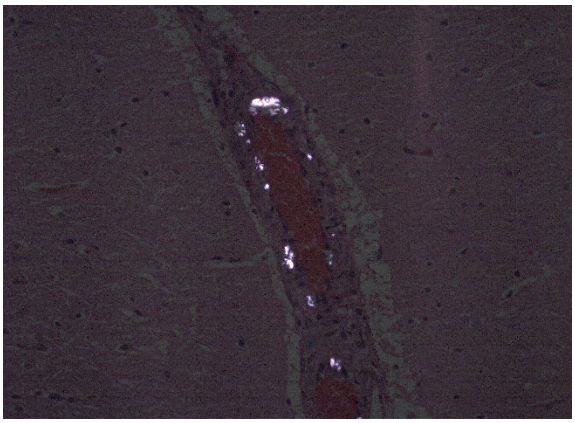

Figure 2-6. Cerebrum, cat: Polarized light enhances the visualization of calcium oxalate crystals in vessel walls. (HE, 100X) (Photo courtesy of: Faculty of Veterinary and Agricultural Sciences, The University of Melbourne, 250 Princes Highway, Werribee Vic 3030, https://www.u-vet.com.au/)

medication in liquid form, particularly for children who were afflicted with sore throats caused by streptococcal infections. The company's chief chemist and pharmacist found sulfanilamide readily dissolved in ditheylene glycol. A pink raspberry-flavored formulation consisting of 10% sulfanilamide, 83% diethylene glycol, and 17% water was formulated. The company laboratory tested the mixture for flavor, appearance, and fragrance. Found to be satisfactory, the product was branded as "Elixir Sulfanilamide". The medication was immediately compounded and 744 shipments (350 gallons in total) were distributed throughout the United States in September 1948. The toxicity of each ingredient was never tested, nor was it required by law.[8]

45 children and 81 adults died due to acute kidney failure out of the 464 individuals confirmed to be exposed to the medication. Early clinical symptoms included nausea, vomiting, and severe abdominal pain, which led many of the survivors to discontinue the medication. Later symptoms included manifestations of renal failure such as polyuria, anuria, flank pain, coma, and seizures.[8] The events associated with Elixir Sulfanilamide facilitated the passage of the 1949 Food,

Drug, and Cosmetic Act. In addition to requiring toxicity of new drugs to be tested prior to marketing, the new law also banned dangerous drugs, false and mis-leading labeling, and required formula disclosures of all active ingredients. Unless the drug was sold by prescription, directions were required for use and in addition to warnings about possible misuse.[8]

The new law was not without its limitations. Proof of efficacy and animal testing were not required and human trials were not always properly executed. In addition, if the FDA failed to consider a drug within 70 days, it was automatically approved.[8]

Nearly a quarter of a century later, thalidomide entered the market in Europe, Australia, and Canada as a sedative and anti-nausea medication for pregnant women. Unbeknownst at the time, the medication was a teratogen and resulted in 6,000 babies born with birth defects. These effects were not seen in the United States due to a FDA medical officer named Dr. Frances Kelsey. Dr. Kelsey's decision to not approve the medication was not in regard to teratogenicity, but instead due to concerns about peripheral neuropathy. Nonetheless, thalidomide's deleterious effects were not seen in the United States due to regulations stemming from the Elixir Sulfanilamide incident.[8]

The FDA's current investigational new drug process requires comprehensive animal testing before initiating extensive human trials. In addition, time constraints for the disposition of new drug applications were removed, effectively transitioning the FDA from an agency that responded to events, as with the Elixir Sulfanilamide incident, to an agency that actively scrutinizes development of new medications.[8]

References:

1. Amoroso L, Cocumelli C, Brozzi A, Tancredi F, Grifoni G, Mastromattei A, Meoli R, Di Guardo G, Eleni C. Ethylene glycol toxicity: a retrospective pathological study in cats: *Veterinaria Italiana* 2017; 54 (4) 251-255.
2. Ciancolo RE, Mohr FC. Urinary system. In*:* Maxie MG, ed. *Jubb, Kennedy and Palmer's Pathology of Domestic Animals*. Vol 2. 6th St. Louis, MO: Elsevier; 2016:425-6.
3. Davis DP, Bramwell KJ, Hamilton RS, Williams SR. Ethylene glycol poisoning: case report of a record-high level and a review. *Journal of Emergency Medicine*. 1997;15(5):654–667.
4. Froberg K, Dorion RP, McMartin KE. The role of calcium oxalate crystal deposition in cerebral vessels during ethylene glycol poisoning. *Clinical Toxicology*. 2006;55.
5. Goldstein RE, N Saisindhu, Sabet N, Goldstein O, McDonough SP. Primary Hyperoxaluria in Cats Is Caused by a Mutation in the Feline GRHPR Gene. *Journal of Heredity*. 2009. Vol 100 pp S2-S7.
6. Lakind JS, McKenna EA, Hubner RP, Tardiff RG. A Review of the comparative Mammalian Toxicity of Ethylene Glycol and Propylene Glycol. *Critical Reviews in Toxicology* 2008; 29:5, 441-465.
7. Moore MM, Kanekar SG, Dhamija R, Ethylene Glycol Toxicity: Chemistry, Pathogenesis, and Imaging. *Radiology Case Report* 2008: 4(1): 122.
8. Paine MF. Therapeutic disasters that hastened safety testing of new drugs. *Clin Pharmacol Ther*. 2017;101(4):430-434.
9. Schweighauser A, Francey T. Ethylene glycol poisoning in three dogs: Importance of early diagnosis and role of hemodialysis as a treatment option: *Fallberichte | Case reports* 2015; DOI 10.17246/sat00051.

CASE III: N14-0235 (JPC 4137405).

Signalment:
14-year-old Hereford bull (*Bos taurus)*

History:
The bull presented to the referring veterinarian for a swollen left eyelid and a mass ventral to the left ear. On presentation, there was marked corneal edema and ulceration of the left eye, and areas of alopecia were noted on the ventral midline skin. Histopathology of the eyelid was consistent with squamous cell carcinoma. The bull was euthanized and a full necropsy was performed.

Gross Pathology:
At necropsy, multiple areas of circular, crusting alopecia were in a line along the ventral midline skin cranial to the prepuce. The largest lesion was 8 cm in diameter and the smallest was 3 cm. Additional gross lesions included squamous cell carcinoma of the left eye and enlarged mandibular lymph nodes.

Laboratory results:
No laboratory results reported.

Microscopic Description:
Two sections of haired skin from the ventral abdomen of the bull are submitted. There may be slide variation. Throughout the superficial and mid dermis centered around multifocal hair follicles and blood vessels, is an inflammatory infiltrate composed of numerous eosinophils and macrophages with fewer lymphocytes and plasma cells. Inflammation frequently surrounds sweat glands and diverticula at the hair follicle base that often contain cross-sections of 100 µm in diameter adult, filariid nematodes that have a 5 µm-thick, smooth cuticle, a pseudocoelom, polymyarian-coelomyarian musculature, lateral alae, prominent intestine, and either

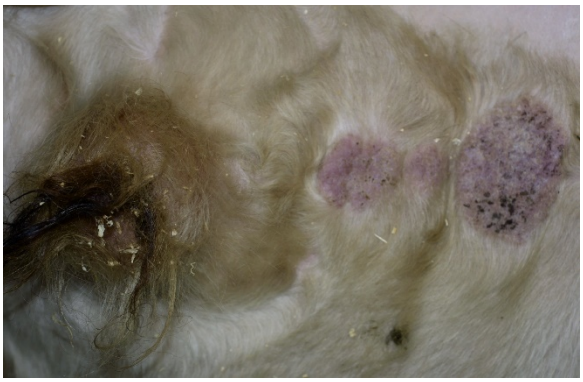

Figure 3-1: Multiple areas of circular, crusting alopecia were in a line along the ventral midline skin cranial to the prepuce. (Photo courtesy of: Texas A&M University, College of Veterinary Medicine & Biomedical Sciences, Department of Veterinary Pathobiology, 660 Raymond Stotzer Pkwy, College Station, TX 77843, https://vtpb.tamu.edu/)

paired uteri containing microfilariae and eosinophilic discs or a testis. Occasionally, nematodes and necrotic debris are surrounded by multinucleate giant cells, and follicle diverticula are ruptured and replaced by similar inflammation and necrotic debris (furunculosis). There is mild, diffuse loss of adnexal glands, and hair follicles are frequently dilated with attenuated epithelium and abundant keratin, and occasional contain degenerate neutrophils and necrotic debris within the lumen or epithelium (folliculitis). Multifocally, the remaining apocrine glands are ectatic and there is increased connective tissue and small-caliber blood vessels (fibrosis). A few areas of hemorrhage, fibrin, and edema in the congested superficial dermis. The epidermis is moderately hyperplastic with formation of rete ridges, mild orthokeratotic and parakeratotic hyperkeratosis, spongiosis, and acanthosis. A few intracorneal pustules characterized by degenerate eosinophils, neutrophils and cellular debris embedded in proteinaceous fluid and containing rare nematodes and superficial bacteria are throughout the sections.

Contributor's Morphologic Diagnoses:
Skin: moderate, multifocal, chronic

eosinophilic and histiocytic dermatitis, folliculitis, and furunculosis with intralesional filarial nematodes (*Stephanofilaria stilesi*, presumed).

Contributor's Comment:

While considered an incidental lesion in this case, stephanofilariasis is a common cause of dermatitis in cattle (particularly beef breeds) in the western and southwestern United States.[4,5] The genus *Stephanofilaria* (Order *Spirurida*, Family *Filariidae*) encompasses several species of filariid nematodes that infect the skin of cattle and buffalo worldwide and are also found on goats, elephants, and rhinoceroses.[3,5] Lesion distribution is often dependent on the feeding preference of the fly vector that transmits the parasite,[3,5] with some species primarily causing lesions on the back ("hump-sore" of Zebu cattle; *S. assamensis*) or shoulder (*S. dinniki* in rhinoceroses), ears (*S. zaheeri* in buffalo), or feet (*S. kaeli*).[3,5] Speciation can be difficult due to subtle differences between species, erroneous taxa,[3] and a lack of comparative genomic analyses within the genus. In North America, the primary species is *S. stilesi*, which is transmitted by horn flies (*Haematobia irritans*) that ingest micro-filariae and deposit infective larvae while

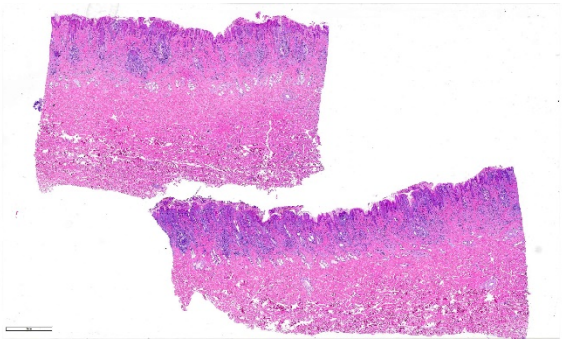

Figure 3-2: Haired skin, ox. Two sections of skin with marked acanthosis and hyperkeratosis are submitted for examination. (HE, 5X)

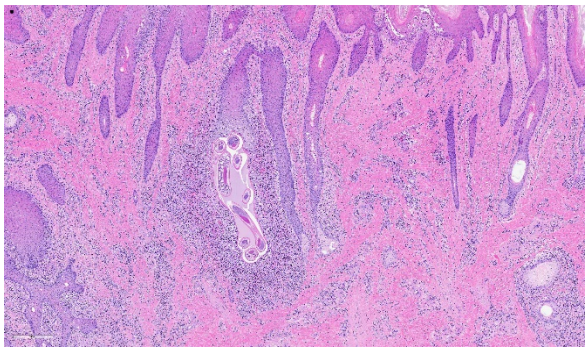

Figure 3-3: Haired skin, ox: Multiple cross sections of an adult nematode are present within this inflamed follicle. There is marked acanthosis of the overlying skin (HE, 192X)

feeding on the skin.[5] The characteristic gross finding, as observed in this case, is development of singular or multiple alopecic and lichenified plaques along ventral midline.[5] Similar lesions may also occur on the scrotum, flank, udder, or teats.[5] Differential diagnoses for cutaneous nematodiasis in cattle would include infection with *Rhabditis* spp., *Onchocerca* spp., or rarely *Pelodera* spp.[4,5]

Histologically, adult *S. stilesi* reside in cystic diverticula off the base of hair follicles and microfilariae can be found on the skin surface enclosed in vitelline membranes, free within the dermis, or within lymphatic vessels.[3,5] Inflammatory reaction to the adult nematodes is mild unless there is rupture of the cyst wall and spread to the dermis, where the cellular reaction is mainly eosinophilic or lymphocytic.[3,5] Adult filariid nematodes are characterized by a thick cuticle, coelomyarian musculature, thick-walled intestine, lateral alae, and paired uteri containing microfilariae and eosinophilic discs in the female.[2] *S. stilesi* infections can be differentiated from *Pelodera* spp. by the presence of microfilariae in the uteri, a prominent intestine, and absence of a

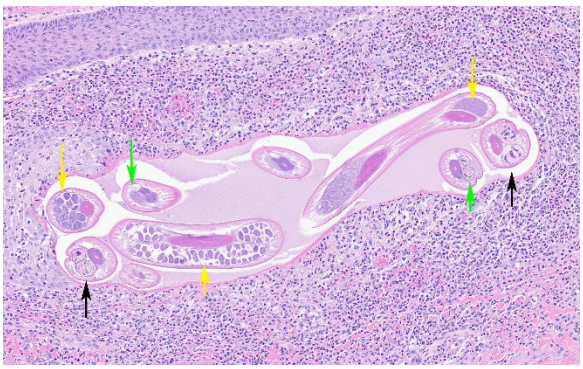

Figure 3-4: Haired skin, ox: Adult females demonstrate paired uteri with ova (yellow arrows), uteri with filarid larva (black arrows) and a single testis (green arrows) (HE, 387X).

rhabditiform esophagus.[2,4] *Rhabditis* is another rhabditiform nematode genus that is most often associated with otitis externa in cattle and can exhibit matricidal hatching in which the larvae feed on the maternal tissues after developing in the uterus.[1] *Onchocerca* spp. adults are not found in the hair follicles and the microfilariae are longer (200 µm vs. 50 µm) than *S. stilesi*.[3,4] Stephanofilariasis is often mild, but if treatment is desired, the parasite can be killed effectively with ivermectin or topical organophosphates.[4]

Contributing Institution:

Texas A&M University
College of Veterinary Medicine & Biomedical Sciences
Department of Veterinary Pathobiology
660 Raymond Stotzer Pkwy, College Station, TX 77843
https://vtpb.tamu.edu/

JPC Diagnosis:

Haired skin: Dermatitis, perifollicular, periadnexal and perivascular, eosinophilic and histiocytic, diffuse, moderate, with folliculitis, furunculosis, few intrafollicular adult filarid nematodes, and rare dermal microfilariae

JPC Comment:

The contributor provides a concise overview of the genus *Stephanofilariae* in addition to other etiologic agents that cause cutaneous nematodiasis in domestic and wildlife species.

As briefly mentioned by the contributor, rhinoceroses are one of the many species affected by this genus. Black rhinoceroses (*Diceros bicornis)* have been known to be infected by *Stephanofilaria dinniki*[7], although a 2012 case report describing a filariosis outbreak in Meru National Park in Kenya described lesions consistent with the parasite in both black rhinoceroses and southern white rhinoceroses (*Ceratotherium simum simum)*.[6]

Macroscopically, lesions were characterized by extensive cutaneous ulcerations with a 2-3cm depression and a mean diameter of 23 ±8cm in in white rhinoceroses. Similar lesions of black rhinoceroses but were smaller, measuring 15 ±5cm in diameter. Unfortunately nematodes were not observed in tissue samples obtained for histo-morphologic examination; however, the authors attributed the filarid-like lesions to *S. dinniki* due to a striking resemblance to previously reported lesions caused by the parasite in addition to resolution following treatment with ivermectin.[6] Although the lifecycle of *S. dinniki* is unknown, other species within the genus (such as S. *stilesi*) require a blood sucking arthropod vector, of which several species are commonly found on rhinoceroses and are thought to be involved in the parasite's transmission. In addition, a species of bird commonly observed in association with African megafauna, commonly known as oxpeckers, were also observed pecking at the lesions. The relationship between these large mammals and oxpeckers is usually classified as a "cleaning symbiosis" as each species

benefits from the other under normal circumstances.

Although the act of oxpeckers feeding on necrotic skin is inherently traumatic, the authors suggest this may be beneficial from an epidemiological standpoint. This action likely disrupts the parasite's lifecycle by preventing arthropod vectors from ingesting microfilaria concentrated within the necrotic and infected cutaneous tissues.[6] Of note, microfilaria were not observed by all participants due to slide variation.

References:

1. Duarte ER, Hamdan JS. Otitis in Cattle, an Aetiological Review. *Journal of Veterinary Medicine, Series B*. 2005;51: 1-7.
2. Gardiner CH, Poynton SL. *An atlas of metazoan parasites in animal tissues.* C.L. Davis Foundation; 2006.
3. Johnson SJ. Stephanofilariasis- a review. *Helminthological Abstracts, Series A (Animal and Human Helminthology)*. 1987;56: 287-299.
4. Klei TR. Helminths of the skin. In: Kahn CM, ed. *Merck Veterinary Manual*. 10 ed. Kendallville, Indiana: Courier Kendallville, Inc.; 2010:826-840.
5. Mauldin EA, Peters-Kennedy J. Integumentary System. In: Maxie MG, ed. *Pathology of Domestic Animals*. 6 ed. China: Elsevier; 2016:686-687.
6. Mutinda M, Otiende M, Gakuya F, et al. Putative filariosis outbreak in white and black rhinoceros at Meru National Park in Kenya. *Parasit Vectors*. 2012;5:206.
7. Tremlett, JG. Observations on the pathology of lesions associated with *Stephanofilaria dinniki* round, 1964 from the black rhinoceros (*Diceros bicronis*). *J Helminthol. 1964; 38:171-174.*

CASE IV: WSC CASE 2 (JPC 4155410)

Signalment: Sixteen-year-old, male, cynomolgus monkey (*Macaca fascicularis*)

History: Over a 2-year period this monkey had variable increased body weight (BW) of up to 3 kilograms (kgs) greater than his original BW of 7 kgs. The following year, this monkey lost 13% of his body weight. The clinical chemistry evaluation showed significant increases in serum and urine glucose (Glu), as well as in serum triglycerides (Trigl), cholesterol (Chol) and decreases of potassium (K). There were also minimal increases in alanine amino-transferase (ALT) and aspartate amino-transferase (AST). Although this monkey had no changes in appetite or mental faculties, he was euthanized because of clinical signs of Type 2 diabetes mellitus (T2DM). All procedures were approved by the animal care and use committee in accordance with federal regulations and the Guide for the Care and Use of Laboratory Animals.

Gross Pathology: At necropsy, there were no gross findings.

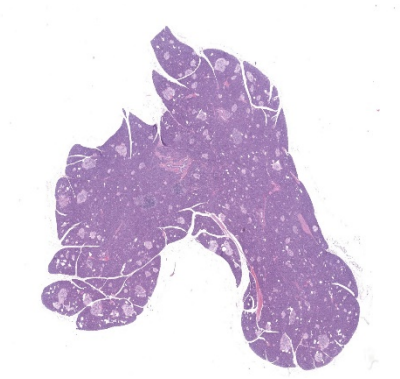

Figure 4-1: Pancreas, cyno macaque. A section of pancreas is submitted for examination. At subgross magnification, islets are increased both in size and number. (HE, 7X)

	Serum				Urine	Body weight
	Glucose	**Cholesterol**	**Triglycerides**	**Phosphorus**	**Glucose**	
Date/Range	**42-157 mg/dL**	**20-91 mg/dL**	**69-139 mg/dL**	**3.7-7.8 mg/dL**	**mg/dL**	**~ 8 kg**
2017	59-74	39-154	66-96	4.6-4.9	NE	8-8.4
2018	78-137	**104-177**	79-80	3.7-4.5	NE	**8.3-10**
2019	**295-501**	**933-1568**	104-**207**	**2.8-3.4**	**>1000**	**7.7**

Table 1: Clinical pathology parameters and total body weights taken in this monkey from 2017 to 2019. Bolded red values are significant changes. NE= No evaluated.

Samples of adrenal, aorta, brain, gall bladder, heart, kidneys, liver, lung, pancreas, sciatic nerve, skin, spleen, ureters, and urinary bladder were collected and fixed in 10% neutral buffered formalin; eyes and optic nerves were fixed in Davidson's solution. These tissues were processed to slides and stained with Hematoxylin and eosin (HE) for light microscopic examination.

Laboratory results: Table 1 is showing clinical chemistry parameters from 2017-2019 taken for this monkey. At the time of euthanasia, there were marked increases blood Glucose (295-501 mg/dL), urine Glucose (> 1000 mg/dL) and Chol (933-1568 mg/dL) and increases in and Trig= (104-207 mg/dL). Insulin and hemoglobin A1c were not evaluated.

Microscopic Description: Pancreatic islets of Langerhans displayed several different histopathologic alterations. These included islet cell hyperplasia/hypertrophy, degeneration, necrosis and loss; accumulation of intracellular and extracellular pale, eosinophilic, irregularly shaped material (amyloid); and mononuclear cell infiltrate (lymphocytes). Islet cell hyperplasia/ hypertrophy was characterized by increased numbers of enlarged cells with large prominent nuclei arranged in acini formations. Degenerating islet cells had vacuolated cytoplasm or contained large amounts of intracytoplasmic amyloid. Necrotic cells had pyknotic to karyorrhectic nuclei. There were also several small islets that contained mostly extracellular amyloid and a few cells. A few islets of Langerhans contained variable numbers of mononuclear cells (lymphocytes). The eosinophilic material was not birefringent when the HE and Congo Red stained slides of pancreas were placed under polarized light but was still considered to be consistent with amyloid.

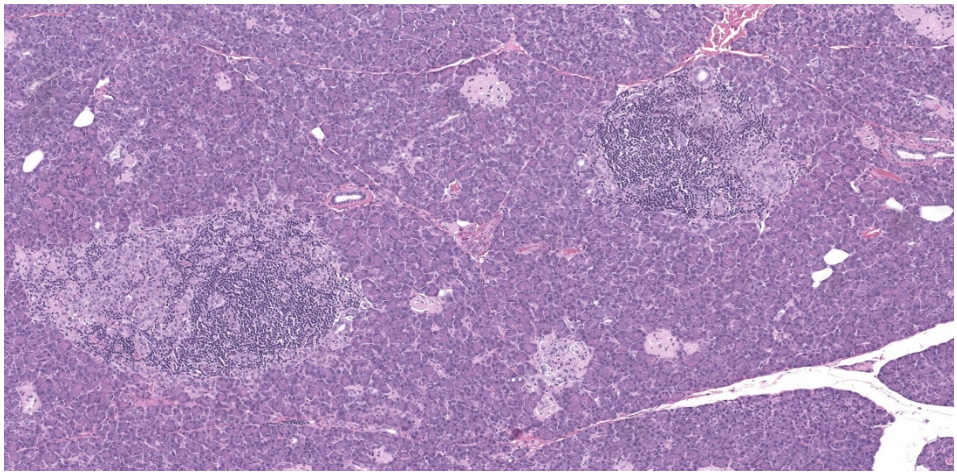

Figure 4-2: Pancreas, cyno macaque. Some enlarged islets are infiltrated by large numbers of lymphocytes (insulitis) (HE, 81X).

To further characterize the pancreatic lesions, immunehistochemical stains for Insulin (Dako

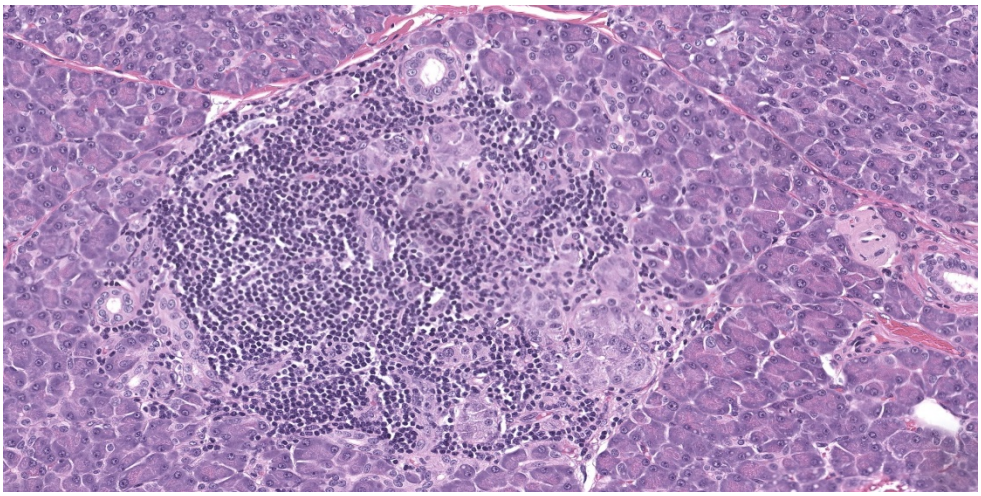

Figure 4-3: Pancreas, cyno macaque. Higher magnification of an islet infiltrated by large numbers of lymphocytes

guinea pig anti-Insulin A0564 1/7, 500, 20' @ RT) and glucagon (Abcam anti-glucagon ab-92517 1/20,000 15' @ RT) were performed on the pancreas of this monkey and from in internal control insulin stains for beta cells demonstrated moderate to marked decreases in expression in the reported monkey as compared to the control monkey. Glucagon stains for alpha cells in the reported monkey were in-conclusive because the control pancreas contained a large percentage cells that were positive for glucagon, likely due to antigen cross reactivity.

Other microscopic findings included multifocal cortical infarcts and multifocal glomerulopathy in the kidneys, and focal extensive, moderate interstitial fibrosis with cardiomyocyte loss and hypertrophy in the heart.

There were no microscopic findings in the adrenal glands, aorta, brain, gall bladder, liver, lung, sciatic nerve, skin, spleen, ureters and urinary bladder.

Contributor's Morphologic Diagnoses: Pancreas, islets of Langerhans: Hyperplasia/ hypertrophy, degeneration/ necrosis, and mononuclear infiltrate

Pancreas, islets of Langerhans: intra-cellular and extra-cellular amyloid accumulation, marked, multifocal to diffuse

Pancreas-, Islets of Langerhans: De-creased immune-histochemical insulin expression

Kidneys – Cortical infarcts, chronic, multifocal and glomerulopathy

Heart – Fibrosis and cardiomyocyte loss and hyper-trophy of the left myocardial wall, moderate and focally extensive

Contributor's Comment: The clinical history of increases in BW followed by sig-nificant decreases of BW and the age of this monkey, as well as the alter-ations in the clinical pathology parameters and microscopic find-ings in the pancreas are all consistent with T2DM.

Factors such as obesity, sedentary lifestyle, and an increased in aging population have increased the prevalence of T2DM in humans around the world.[3] Nonhuman primates (NHPs), as well as cats, dogs, and pigs also develop spontaneous type 2 diabetes mellitus (T2DM) so they are used as animal models.[5] Though, they do not develop all the characteristics of T2DM in humans, they can be used to study some specific con-ditions.[3] Depending on the stage of disease, T2DM is characterized by obesity, glucose intolerance, insulin resistant, dyslipidemia, hypertension, inflammatory processes, abnormalities of the blood coagulation system and/or pancreatic pathology.[3]

In NHPs, T2DM has been described in both old and new-world monkeys.[1,2,4,6,10,12,13,16] The most extensive research has been conducted in cynomolgus and rhesus macaques.[5] In NHPs, spontaneous T2DM increases in incidence and severity with age and increased in body weight.[1, 15] Wagner et al., 2001[14] reported that approximately 30% of cynomolgus macaque 15 years of age or older had evidence of T2DM.

T2DM in humans and animal models is characterized by the following phases: Normal glucose tolerance followed by insulin resistant due to compensatory increases in insulin secretion plus alterations of carbohydrate metabolism. The disease progresses to impaired glucose with increases in fasting plasma glucose. Hyperglycemia due to decreases of insulin production caused by pancreatic pathology.[3,6,14]

Cynomolgus macaques are typically overweight early on in the course of the disease and as the disease gets more severe they lose weight. They also exhibit clinical chemistry alterations (increased total cholesterol, triglycerides, and free fatty acids as well as decreased HDL cholesterol), inflammation and increased blood pressure.[15]

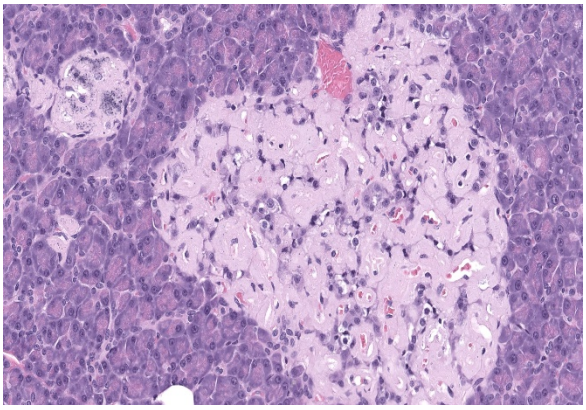

Figure 4-4: Pancreas, cyno macaque. Higher magnification of an islet effaced by large amounts of amyloid. (HE, 270X)

The microscopic findings of T2DM in humans and NHPs include hyperplasia and hypertrophy of β cells because the pancreas responds to peripheral insulin resistance by increasing insulin production.[9,11,13,14,15,16,17] As the insulin demands continue, there is co-secretion of Amylin (islet amyloid polypeptide or IAPP), resulting in intracellular accumulation within the Islets. Aggregated IAPP has cytotoxic properties causing degeneration, necrosis and loss of β cells, resulting in release of the amyloid. Infiltration of mononuclear cells is not uncommon, secondary to cellular destruction. As these lesions progress, the remaining (Alpha, delta, pancreatic polypeptide, epsilon) pancreatic cells undergo degeneration and necrosis

It is important to mention the cell types present in pancreatic Islets and what they secrete.[8] Alpha cells produce Glucagon. Glucagon stimulates glycogenolysis, gluco-neogenesis, and lipolysis. Beta cells produce insulin and islet-amyloid poly-peptide (IAPP - amylin). Insulin stimulates glucose uptake and glycogenesis in response to hyperglycemia. Insulin is also an anabolic hormone released by beta cells in response to glucose and other nutrients such as amino acids, fatty acids and hormones. Amylin suppresses glucagon production and inhibits gastric digestive function. Delta cells produce somatostatin. Somatostatin inhibits release of glucagon, insulin and pancreatic polypeptide. PP cells produce pancreatic polypeptide. Their function is to antagonize cholecystokinin. Cholecystokinin inhibits exocrine pancreas secretion and gall bladder contraction and delays gastric emptying. Epsilon cells produce ghrelin. This hormone stimulates the appetite and suppresses insulin secretion.

With immune-histochemical staining we observed remarkable decreases in insulin

staining in the pancreatic islets if our 16-year old monkey, compared to a control. In 1986, Howard and Bueren[7] performed computerized photometric method on immune-histochemically stained, Insulin (β cells), glucagon (α cells) and somatostatin (δ cells) cells in the pancreas of nondiabetic (ND), hormonally impaired, borderline diabetic (D) and diabetic of *Macaca nigras*. He found alterations in percentages of secretory cells correlated with several of the metabolic and clinical changes. These consisted of decreases of insulin from 77% in ND to 1% in D monkeys. Glucagon and somatostatin stains also decreased in the D monkeys but in a lower degree, as percentage of these cells is normally lower in the pancreas.

Kidney and heart findings are common aged-related findings in older monkeys.

Contributing Institution:
Pfizer Drug Research and Development
455 Eastern Point Rd
Groton, CT 06340

JPC Diagnosis:
1. Pancreas, islets: Hyperplasia, diffuse, moderate with islet cell hypertrophy and rare tubuloinsular complexes (nesidioblastosis).

2. Pancreas, islets: Amyloidosis, diffuse, severe.

3. Pancreas, islets: Insulitis, lymphocytic, multifocal, moderate.

JPC Comment: The contributor expertly summarizes the pathogenesis, clinical findings, and nuances associated with T2DM in NHPs, which closely mirror those of humans. The prevalence of T2DM has significantly increased amongst people throughout the world and the trend will likely continue for the foreseeable future.[3] In addition to characteristic features provided by the contributor (e.g. obesity, hypertension), human patients with T2DM are predisposed to two neurodegenerative diseases in which misfolded amyloidogenic peptides play pivotal roles, Alzheimer's disease and Parkinson's disease. Ongoing research has found insulin-degrading enzyme (IDE) to be a link between T2DM and these two diseases.[12]
IDE has degradative activity over insulin, playing a central role in its clearance and regulation, and therefore overall homeostasis. First demonstrated in mice with an ablated *Ide* gene, its absence or loss of function results in hyperinsulinemia and contributes to the development of T2DM.[12]
In addition to degrading insulin, IDE interacts with and degrades a wide spectrum of substrates, including islet amyloid polypeptide (IAPP, also known as amylin) and

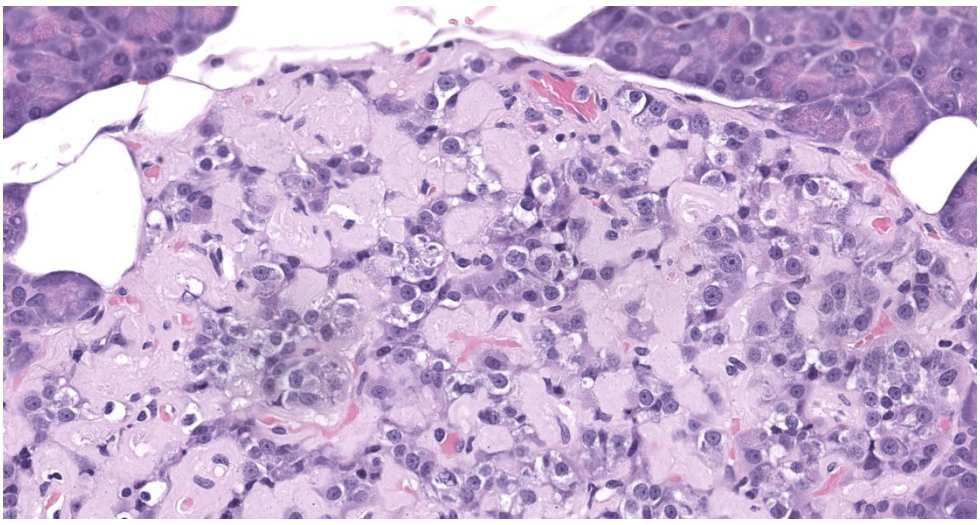

Figure 4-5: Pancreas, cyno macaque. Islet cells within amyloid-producing islets are swollen and vacuolated (degeneration) or shrunken with pyknotic nuclei (necrosis) (HE, 380X)

amyloid-β (Aβ) peptides, which have the ability to undergo conformational change and form β-sheets. Furthermore, the enzyme is concentrated in tissues where amyloidogenic risk is elevated, such as pancreatic β cells and the brain, which are continuously challenged with IAPP and Aβ aggregation, respectively. One way IDE prevents formation of these aggregates is by exhibiting chaperone-like activity over amyloidogenic peptides and facilitating proper folding, including amyloidogenic peptides related to neurodegenerative diseases, such as Aβ in the case of Alzheimer's disease and α-synuclein, which plays a pivotal role in the development of Parkinson's disease.[12] T2DM's association with the development of Alzheimer's disease and Parkinson's disease is potentially tied to hyperinsulinemia, which occurs in the early stages in the disease process as described by the contributor. High levels of insulin may overwhelm IDE, resulting in favorable conditions for the aggregation of amyloid-ogenic peptides.[12]

Given its association with these three entities, IDE is an enticing target for medicinal research, although challenges, such as those due to toxicity (e.g. hypoglycemia) must be overcome.[12]
During the conference, participants noted what the contributor described within rare islets as hyperplastic and hypertrophic cells arranged in acini formations. The moderator discussed how this finding is consistent with nesidioblastosis given that neither acini nor tubular structures are normally present in these locations.

Nesidoblastosis is a non-neoplastic pro-liferation of islet and ductular tissue within the pancreas that is histologically char-acterized by irregularly sized islets, hypertrophied β cells, and ductulo-insular complexes ("insulo" referring to islet cells including but not limited to, insulin producing β cells).[5] The pathogenesis of nesidioblastosis is unclear; it occurs as both a regenerative response to pancreatic insults and in response to increased β cell trophic factors, such as T2DM.

Nesidioblastosis is the most common cause of hyperinsulinemic hypoglycemia in humans.[5] However, nesidioblastosis is sporadically reported in domestic species, particularly in dogs, and is typically an incidental finding.[8]

References:

1. Cai G, Cole SA, Tejero ME, Proffitt JM, Freeland-Graves JH, Blangero J, Comuzzie AG. Pleiotropic effects of genes for insulin resistance on adiposity in baboons. *Obes Res*. 2005;12(11):1866–72.
2. Cann JA, Kavanagh K, Jorgensen MJ, Mohanan S, Howard TD, Gray SB, Hawkins GA, Fairbanks LA, Wagner JD. Clinico-pathologic characterization of naturally occurring diabetes mellitus in vervet monkeys. *Vet Pathol.* 2010;57(5):714–8.
3. Cefalu WT, Animal Models of Type 2 Diabetes: Clinical Presentation and Pathophysiological Relevance to the Human Condition, *ILAR Journal*, Volume 57, Issue 4, 2006, Pages 186–198
4. Comuzzie AG, Cole SA, Martin L, Carey KD, Mahaney MC, Blangero J, VandeBerg JL. The baboon as a nonhuman primate model for the study of the genetics of obesity. *Obes Res*. 2004;11(1):75–80.
5. Gacar A, Pekmezci D, Karayigit MO, Kabak YB, Gulbahar MY. Nesidioblastosis in a simmental calf. *J Comp Pathol*. 2012;147(4):491-494.

6. Harwood HJ Jr, Listrani P, Wagner JD. Nonhuman primates and other animal models in diabetes research. *J Diabetes Sci Technol*. 2012;6(4):504–515.
7. Howard CF. Diabetes in Macaca nigra: metabolic and histologic changes. *Diabetologia*. 1975 Nov 1;10(1):671-7.
8. Howard CF Jr, Van Bueren A. Changes in islet cell composition during development of diabetes in Macaca nigra. *Diabetes*. 1986;45(2):165-181.
9. Jubb KFV, Stent AW. Pancreas. In: *Jubb, Kennedy, and Palmer's Pathology of Domestic Animals* Maxie, M Grant. Sixth edition. St. Louis, Missouri: Elsevier, 2016. 2:370-3.
10. Palotay JL, Howard CF: Insular Amyloidosis in Spontaneously Diabetic Nonhuman Primates, *Vet Pathol.* 1982;19 (Suppl 7):181-192.
11. Pirarat N, Kesdangsakolwut S, Chotiapisitkul S, Assarasakorn S. Spontaneous diabetes mellitus in captive Mandrillus sphinx monkeys: a case report. *J Med Primatol.* 2008;47(4):162–5.
12. Sheldon, W. G., & Gleiser, C. A. (1971). Amyloidosis of the Islets of Langerhans in a Crab-Eating Monkey (Macaca fascicularis). *Veterinary Pathology*, 8(1), 16–18.
13. Sousa L, Guarda M, Meneses MJ, Macedo MP, Vicente Miranda H. Insulin-degrading enzyme: an ally against metabolic and neurodegenerative diseases [published online ahead of print, 2021 Aug 16]. *J Pathol*. 2021;10.1002/path.5777.
14. Tardif SD, Power ML, Ross CN, Rutherford JN, Layne-Colon DG, Paulik MA. Characterization of obese phenotypes in a small nonhuman primate, the common marmoset (callithrix jacchus). *Obesity (Silver Spring)*. 2009;18(8):1599–505.
15. Wagner JD, Cann JA, Zhang L, Harwood HJ Jr. Diabetes and obesity research using nonhuman primates. In: Abee CR, Mansfield K, Tardif SD, Morris T, eds. *Nonhuman primates in biomedical research Volume 2: Diseases*. 2nd ed. 2012. Elsevier. Chapter 15, pp 699–742
16. Wagner JD, Cline JM, Shadoan MK, Bullock BC, Rankin SE, Cefalu WT. Naturally occurring and experimental diabetes in cynomolgus monkeys: a comparison of carbohydrate and lipid metabolism and islet pathology. *Toxicologic pathology*. 2001 Jan;29(1):152-8.
17. Wagner JD, Kavanagh K, Ward GM, Auerbach BJ, Harwood HJ Jr, Kaplan JR, Old World Nonhuman Primate Models of Type 2 Diabetes Mellitus, *ILAR Journal*, Volume 57, Issue 4, 2006, Pages 259–271.
18. Westermark P. Amyloid in the islets of Langerhans: thoughts and some historical aspects. *Upsala journal of medical sciences.* 2011 May 1;116(2):819
19. Westermark P, Andersson A, Westermark GT. Islet amyloid polypeptide, islet amyloid, and diabetes mellitus. *Physiological reviews*. 2011 Jul;91(4):795-826.